

See discussions, stats, and author profiles for this publication at: <https://www.researchgate.net/publication/311100889>

Direct emissions of nitrous oxide from combustion of gaseous fuels

Article in *International Journal of Hydrogen Energy* · January 2016

DOI: 10.1016/j.ijhydene.2016.09.202

CITATIONS

2

READS

67

3 authors, including:



Andres Colorado

University of Antioquia

26 PUBLICATIONS **110** CITATIONS

[SEE PROFILE](#)



Vincent Mcdonell

University of California, Irvine

210 PUBLICATIONS **1,934** CITATIONS

[SEE PROFILE](#)

Some of the authors of this publication are also working on these related projects:



Co-combustion of solid/liquid and gaseous fuels [View project](#)



Flashback and Flameholding in Gas Turbine Premixers [View project](#)



ELSEVIER

Available online at www.sciencedirect.com

ScienceDirect

journal homepage: www.elsevier.com/locate/he

Direct emissions of nitrous oxide from combustion of gaseous fuels

Andrés Colorado ^{a,*}, Vincent McDonell ^b, Scott Samuelsen ^b

^a Grupo de Ciencia y Tecnología del Gas y Uso Racional de la Energía (GASURE), Facultad de Ingeniería, Universidad de Antioquia, Calle 67 Número 53 – 108 Medellín, Colombia

^b UCI Combustion Laboratory (UCICL), The Henry Samueli School of Engineering, University of California, Irvine, CA 92697-3550, USA

ARTICLE INFO

Article history:

Received 7 June 2016

Received in revised form

26 September 2016

Accepted 28 September 2016

Available online xxx

Keywords:

Nitrous oxide

N₂O

Gaseous fuels

Ozone depletion

Greenhouse gas

Low-NO_x

ABSTRACT

After molecular nitrogen, nitrous oxide (N₂O) is the second most abundant nitrogen compound in the atmosphere and its concentration is rising at rate of 0.26% yr⁻¹ (0.7 ppb yr⁻¹). In the troposphere N₂O is a relatively stable compound, however it is reactive in the stratosphere, where it is destroyed by photolysis with ultraviolet radiation. While photolysis in the stratosphere removes this potent greenhouse gas from the atmosphere, subsequent reactions also destroy protective ozone. Hence N₂O is both a greenhouse gas and an ozone depleting gas and its increasing levels in the atmosphere warrant further understanding of its sources, including combustion. Most research on combustion generated N₂O has focused on emissions from solid and liquid fuels, since these fuels contain nitrogen bonded to their molecular structure (fuel-nitrogen). It has been shown that this fuel bound nitrogen can be oxidized into N₂O under relatively low temperature conditions. To date, direct emissions of N₂O from combustion of typical gaseous fuels (which have no fuel bound nitrogen) have not received attention due to the established link fuel nitrogen and N₂O emission. This paper presents evidence of alternative mechanisms of N₂O emissions that do not involve fuel bound nitrogen. Of particular interest are lean premixed flames widely used for current low NO_x combustion systems. Measurements were made under different operational modes: Steady state, ignition, and lean blowoff. A variety of gaseous fuel mixtures without fuel nitrogen including natural gas were considered, including, biogas and natural gas with up to 70% H₂ added (by volume). The results indicate that combustion of these fuels can directly emit significant levels of N₂O, in particular during transient events such as ignition and blowoff. Furthermore, steady state combustion of hydrogen enriched natural gas flames (which can be operated at very lean conditions due to the stabilizing effects of hydrogen), can also lead to the direct emissions of N₂O.

© 2016 Hydrogen Energy Publications LLC. Published by Elsevier Ltd. All rights reserved.

Introduction

Nitrous oxide (N₂O) is present in earth's atmosphere at a trace level, yet is the most abundant nitrogen compound in the

atmosphere after molecular nitrogen. The concentration of N₂O is rising at rate of 0.26% yr⁻¹, and its current mixing ratio in air is on the order of 320 parts per billion (ppbv) [1]. This concentration has been increasing linearly over the last few decades as a consequence of the introduction of nitrogen

* Corresponding author.

E-mail addresses: felipe.colorado@udea.edu.co, andresc380@gmail.com (A. Colorado).

<http://dx.doi.org/10.1016/j.ijhydene.2016.09.202>

0360-3199/© 2016 Hydrogen Energy Publications LLC. Published by Elsevier Ltd. All rights reserved.

compounds into the atmosphere at a rate greater than its rate of removal [2,3]. N₂O is one of the long-lived greenhouse gases (CO₂, CH₄ and N₂O) and its global warming potential calculated over a timescale of 100 years is 300 times as potent as CO₂. In the troposphere, N₂O is a relatively stable compound, which allows it to (1) act uninhibited as greenhouse gas (GHG) and (2) be convected into the stratosphere, where N₂O is destroyed by direct photolysis by ultraviolet radiation. The destruction of N₂O, while removing a potent GHG from the atmosphere, cascades into a different environmental problem: NO is formed by reaction with excited atomic oxygen, which causes decomposition of stratospheric ozone (O₃), thus diminishing the protective role of the ozone layer against harmful effects of UV radiation [4].

Currently, the largest source of anthropogenic N₂O is agriculture, driven mainly by the global use of >80 million tons of nitrogen (N) compounds annually as synthetic nitrogen fertilizers, as well as biological nitrogen fixation by leguminous crops [2,5–7]. Natural ecosystems also receive nitrogen compounds as NO_x from fossil fuel and biomass burning, and ammonia (NH₃) from livestock manure. The IPCC estimates that the total N₂O emitted by natural and anthropogenic is around 17.7 Tg N year⁻¹, with 11 and 6.7 Tg N year⁻¹ from natural, and anthropogenic sources, respectively [1]. The IPCC assigns 2 Tg N year⁻¹ to industrial, energy generation and biomass burning processes. Still, the level of uncertainty is large enough and those 2 Tg N year⁻¹ are presented within a lower and higher limit (0.7–3.7 Tg N year⁻¹).

To date, identification of anthropogenic sources has concentrated on (1) industrial processes that may emit globally significant quantities of N₂O, and (2) biological processes that may produce N₂O on a widespread basis. Relative to the consideration of N₂O emissions from combustion of fuels, most of the research in the combustion literature focuses on N₂O emissions from solid and liquid fuels, since these fuels contain nitrogen bonded within their molecular structures (fuel-nitrogen), which can be oxidized into N₂O under relatively low temperature conditions [8–10]. Significant N₂O emissions (>25 ppm_{dv}) have been observed from coal and oil burning power plants, but not from industrial gas flames, even when doped with an equivalent amount of fuel nitrogen [11]. As a result, the literature survey focuses on N₂O emissions from coal fired combustion [8–18]. In particular, fluidized bed coal combustion has been identified as a specific technology that can emit significant amounts of N₂O (25 < N₂O < 85 ppm_{dv}). For comparison, direct emission of N₂O from conventional utility boilers operating on natural gas (NG), residual oil, and pulverized coal have been generally found to be < 6 ppm_{dv} [10]. In relation to the emission of pollutant species from combustion of gaseous fuels, the scientific community has focused its attention mainly on controlling and minimizing the emission of NO_x and products of incomplete combustion (PICs) such as carbon monoxide (CO), unburned hydrocarbons (UHC) and volatile organic compounds (VOC) [19–24]. Similarly the effect of mixing natural gas with hydrogen on the emission of NO_x and CO has been widely studied [25–29]. The relation of these pollutants with the production of photochemical oxidant (i.e., “smog”) is one of the reasons for the widespread interest in NO_x and VOC. These species directly impact on human health due to their role in

formation of tropospheric ozone and fine particulate matter (i.e., PM_{2.5}) [30]. Yet increasing interest in ambient greenhouse gas concentrations motivates examination of other key species such as N₂O which is the focus of the current work.

In terms of the underlying chemistry associated with N₂O emissions, Kramlich and Linak concluded that, in combustion, the homogeneous reactions leading to N₂O are principally NCO + NO → N₂O + CO and NH + NO → N₂O + H, with the NCO reaction being the most important in practical combustion systems. Furthermore, they concluded that any system in which nitrogen containing species are oxidized under relatively low temperatures can emit N₂O. But the possibility of forming N₂O directly from the interaction of N₂ and O₂ during combustion is neglected.

In light of (1) current combustion systems operating at low temperatures to control formation of NO_x, (2) possible increased use of hydrogen allowing even leaner mixtures and stable operation at even lower temperatures, and (3) increasing need/desire to operate combustion systems in a transient manner to follow load and to offset the intermittency of renewable power, a new examination of N₂O from gaseous fuel systems is warranted. As a result, the objectives of the current work are:

- 1) Assess direct emissions of N₂O during ignition and blowoff of gaseous fuels.
- 2) Establish the combustion conditions that favor direct emission of N₂O from gaseous fuels including NG, biogas and those containing hydrogen.

Experiments and methods

Experimental setup

For this study, a confined premixed flame stabilized with a low swirl burner (LSB) was used. A low swirl injector (LSI) was installed inside an optically accessible research boiler and operated on a wide range of gaseous fuel compositions at a fixed fire rate of 117 kW. The LSI is placed in the central axis of the chamber and up-stream of sudden expansion nozzle. The LSI has an overall diameter of 5.1 cm and an inner cylinder diameter of 2.9 cm. Eight (8) swirl-vanes surround the inner cylinder of the LSI at an angle of 37°. The central plane of the LSI has an open area of 2.6 cm², which resulted in a mass flow split ratio between the inner un-swirled and outer swirled region of ~0.3. Given the above parameters and a ratio of radii, R = 0.49, the swirl number (S) for the LSI array is ~0.46. The boiler is mounted on an aluminum table, which is attached to a traverse table allowing movement in all three Cartesian coordinates. The boiler enclosure is shaped as an octagon with sides 30.5 cm wide and 91.5 cm tall made entirely of stainless steel. Eight high temperature VYCOR windows provide optical access to the interior of the combustion chamber. The chamber counts with water-cooled panels used to maintain the walls at a controlled temperature. The cooling water is kept below 311 K with a constant flow rate of 0.56 kg/s. The exhaust stack starts with the same octagonal shape as the walls, but tapers into an octagonal cone with a height of

30.5 cm. The final portion of the stack is a cylinder 20.3 cm diameter and 61 cm height.

Fig. 1 presents a schematic of the LSB fluid dynamics (left) and a photograph of the combustion chamber with annotations showing its main components along with the experimental conditions and measured species (right). The burner consists of swirl vanes in the outer annulus with a perforated plate in front of the inner annulus. Reactants flowing through the injector create a flow field with an outer swirling region with a non-swirling inner region. This creates a divergent flow that generates a decaying velocity profile linearly along the centerline [31]. This characteristic makes the LSB a fuel flexible technology, since it provides a region of locally low reactant velocity that matches the flame speed of multiple fuel compositions without any modification being required. The LSB is a representative low NO_x emissions technology that uses lean premixed combustion to reduce NO_x [32].

Exhaust gas measurements

One contribution to the relatively few studies of N₂O is the lack of convenient/accurate instruments to quantify it. Recently, Quantum Cascade Lasers (QCL) technology has been developed leading to the ability to reliably and stably generate the mid-IR wavelengths at which N₂O can be conveniently and accurately measured using IR Spectroscopy. A Horiba MEXA 1400-QL-NX gas analyzer that utilizes QCL technology was used in the present work to simultaneously measure the concentration of four N-compounds (NO, NO₂, N₂O and NH₃). It is important to highlight that the MEXA 1400-QL-NX analyzer does not use a drying unit to remove the water from the combustion products before the analysis, hence the analyzer reports the concentration of species on a wet basis as part per million (ppm). The MEXA 1400-QL-NX analyzer features a low and a high range for each component as follows:

- N₂O: (Low) 0–5 ppm/50 ppm, (High) 0–200 ppm/2000 ppm
- NO: (Low) 0–10 ppm/100 ppm, (High) 0–500 ppm/5000 ppm
- NO₂ and NH₃: (Low) 0–5 ppm/50 ppm, (High) 0–200 ppm/2000 ppm

The zero and span noise are defined as the standard deviation for concentration reading multiplied by 2. The zero noise

for N₂O and NO is < 0.4 ppm, and < 0.2 ppm for NH₃ and NO₂. The uncertainty for the measurements NO, NO₂, N₂O and NH₃ is 2% of full scale or less. During the experiments the analyzer was set up for readings within the low range. Therefore, the uncertainty for the N₂O and NO₂ measurement is ±0.1 ppm; the uncertainty for the NO measurement is ±0.2 ppm (0–10 ppm) and ±2 ppm (0–100 ppm). Noteworthy is the 10 Hz sampling frequency, which allows some estimation of transient behavior.

An additional analyzer (PG 250 by Horiba) was used to measure NO_x, CO, CO₂, and O₂. The PG-250 utilizes EPA approved measurement methods (1) NDIR (pneumatic) for CO and SO₂, (2) NDIR (pyrosensor) for CO₂; (3) chemiluminescence for NO_x, and (4) a galvanic cell for O₂. The sampling rate for the PG 250 is 1 Hz. The sample probe used to extract exhaust samples is water cooled and located in the exhaust stack. The gases are sent through a condenser unit, drying the sample before entering either analyzer. Before each experiment, the two gas analyzers were calibrated with certified span and zero gases to ensure the most accurate readings.

Additionally, a number of type K thermocouples were placed flush to the inner walls of the boiler to monitor the temperature of different locations.

Experiments

Experiments were carried at atmospheric pressure and without air or fuel preheating (1 bar, ~300 K). Three fuel classes were evaluated: NG, biogas (NG mixed with CO₂ up to 40% by vol.) and NG with up to 70% H₂ by volume. The heat rate into the boiler was fixed at 117 kW. In order to control the air to fuel ratio, only the air flow rate was varied. The LBO limit was achieved by increasing the air flow rate while holding the heat input fixed (117 kW). The variation of the equivalence ratio (ϕ) was simultaneously recorded with the emissions data. ϕ is defined as:

$$\phi = \frac{\text{fuel to oxidizer ratio}}{(\text{fuel to oxidizer ratio})_{\text{stoich}}} = \frac{m_{\text{fuel}}/m_{\text{ox}}}{(m_{\text{fuel}}/m_{\text{ox}})_{\text{stoich}}} \quad (1)$$

NO_x and N₂O were characterized under the following operating scenarios:

- Steady state: the combustion chamber reaches a stable temperature and the heat rate and ϕ are all held constant.

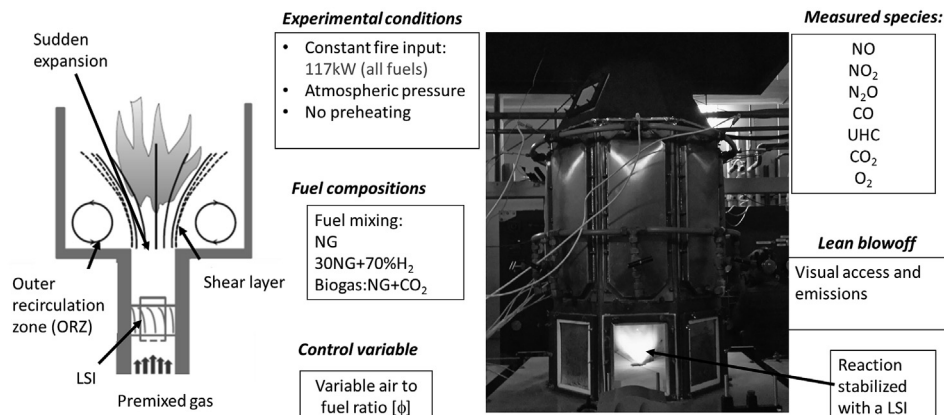


Fig. 1 – LSB schematic flow field (left) and boiler test facility (right).

- Ignition: a spark plug or a pilot hydrogen diffusion flame is used to ignite the reaction. The spark plug or hydrogen pilot is placed perpendicular to the premixed flow direction. The plug or pilot flame is turned off and moved away from the reactions after ignition is completed.
- Blowoff: refers to situations where the flame becomes detached from the location where it is anchored and is physically “blown off”. Blowoff involves the interactions between the reaction and propagation rates of highly strained flames in a high speed, often high shear flow [33].
- Transient ramp for a NG mixed with H₂ (70%H₂-30%NG): at constant firing rate, ϕ was varied from 0.4 to 0.73. This experiment was carried out to observe the effect of the excess of air on the emissions of N₂O.

Correlation analysis

The correlation coefficient among the three nitrogen species (NO, NO₂ and N₂O) was used to establish any relationship between each species, where:

- 1 indicates a strong positive relationship.
- -1 indicates a strong inverse relationship.
- 0 indicates no relationship at all.
- A correlation greater than 0.8 is described as strong, whereas correlations less than 0.5 are described as weak.

Numerical methods

A reactor simulator featuring a perfectly stirred reactor (PSR) in series with a plug flow reactor (PFR), this network of reactors is known as a Bragg cell [34]. CHEMKIN Pro version 15131 was used to solve the gas energy equation. Two reaction mechanisms, GRI 3.0 [35] and the UCSD mechanism [36], were used to calculate trends for N₂O and CO; the experimental emissions of N₂O at LBO are presented for direct comparison.

The fuel used in the model was 100% CH₄. ϕ was varied between 0.5 and 1 with an increment of 0.01. The mass flow rate of premixed gas is a known input variable dependent on ϕ and fire rate. The boundary and initial conditions that define the reactors in the network are as follows:

- PSR: residence time = 1.2 s; pressure = 101.3 kPa; heat loss = 56 kW; temperature (initial guess) = 2000 K.
- PFR: ending position = 5 cm; diameter = 9 cm; heat loss = 10 kW; temperature (initial guess) = 2000 K.

Results and analysis

Steady state experiments with natural gas and biogas

Once the stability was reached, 600 samples of combustion products were continuously measured during 60 s. Fig. 2 compiles the results for NO, NO₂ and N₂O for the combustion of NG at $\phi = 0.8$ and 0.95, Fig. 2a and b respectively. Additionally, Fig. 2c and d show the results for biogas at $\phi = 0.9$ and $\phi = 0.95$, respectively. For ease of comparison, the axes are scaled to the same range of concentrations for each fuel. NO can be read on the left axis and N₂O and NO₂ on the right axis. NO and NO₂ emissions are favored when the premixed gas is close to the stoichiometric point ($\phi = 1$), those conditions entail high reaction temperatures, and higher concentrations of OH radicals and O-atoms, when compared to leaner conditions. For NG, the concentration of NO₂ goes from 0.4 to ~1 ppm, at $\phi = 0.8$ and $\phi = 0.95$, respectively. At $\phi = 0.95$ the emissions of NO₂ are 2.5 times the emissions at $\phi = 0.8$. The emissions of NO go from ~9 to 33 ppm at $\phi = 0.8$ and 0.95, respectively. The emission of NO at 0.95 are around 3.7 times the emissions of NO at $\phi = 0.8$.

Under stable conditions, the measured concentration of N₂O remained under 0.1 ppm regardless of the fuel composition (NG or biogas). These results indicate that, during steady state, the combustion of NG and biogas emits only trace values

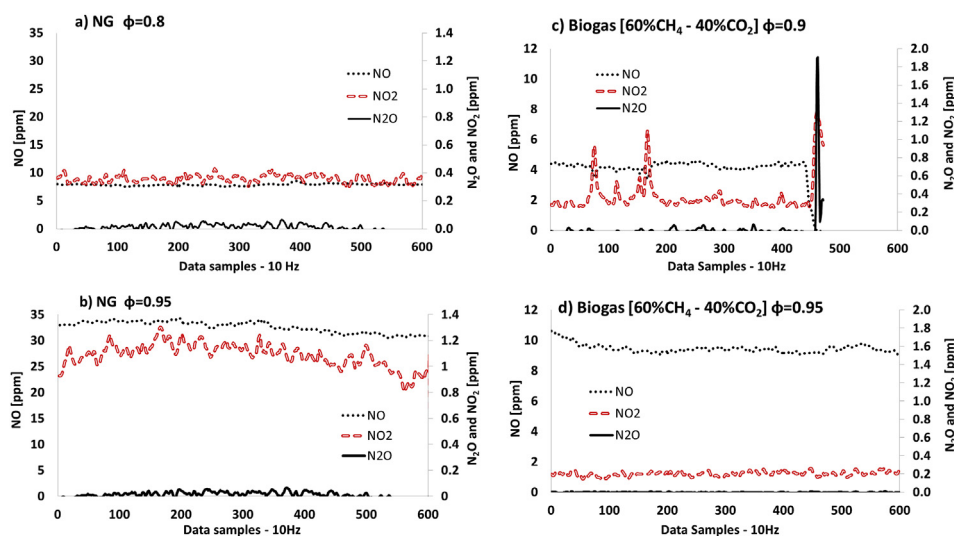


Fig. 2 – On-line exhaust measurements of NO_x and N₂O during steady state operation with NG. a) $\phi = 0.8$, b) $\phi = 0.95$; and biogas 40%CO₂ c) $\phi = 0.9$, d) $\phi = 0.95$.

of $\text{N}_2\text{O} < 0.1$ ppm. For NG, the correlation for $\text{NO}-\text{NO}_2$, $\text{NO}-\text{N}_2\text{O}$ and $\text{NO}_2-\text{N}_2\text{O}$ were 0.73, 0.3 and 0.4, respectively, which indicates only weak positive correlations for the three species. These results are consistent with the conclusion by Kramlich et al. that, in most nitrogen free gas fuel combustion systems, the flame temperature is sufficiently high that any N_2O formed in the flame zone is destroyed before the gases are emitted [9]. However, it is important to emphasize that this conclusion is based on steady state conditions with sufficiently high gas temperatures. It is noted that they concluded that N_2O is a result of the oxidation of fuel–nitrogen at relatively low temperatures which could lead to N_2O emissions. Such conditions can be generated a very lean conditions.

To date, the formation/destruction of N_2O as a by-product has been strongly linked to the gas-phase NO kinetics and more specifically to the transformation of cyanide species into NO and N_2 in the so-called fuel-NO mechanism. The presence of amines or other organic N-compounds in fossil fuels – fuel bound nitrogen – is of paramount importance for the formation of N_2O . Kramlich et al. reported a significant increase in the N_2O concentration by adding nitrogen containing compounds such as ammonia (NH_3), hydrogen cyanide (HCN) and acetonitrile (CH_3CN) to a gas flames in the temperature range 1050–1400 K [11]. Hayhurst and Lawrence provide further evidence that N_2O formation occurs by homogenous gas-phase reaction through the so called NH_i and HCN pathways [37]. The homogeneous reactions leading to N_2O are principally: 1) $\text{NCO} + \text{NO} \rightarrow \text{N}_2\text{O} + \text{CO}$, and to a lesser extent by the reaction: 2) $\text{NH} + \text{NO} \rightarrow \text{N}_2\text{O} + \text{H}$, with the first reaction being the most important in practical combustion systems. The formation of N_2O is, however, counterbalanced by its very fast destruction by hydrogen radicals, according to the reaction: 3) $\text{N}_2\text{O} + \text{H} \rightarrow \text{N}_2 + \text{OH}$.

This conclusion will be revisited for other operational modes and for NG/hydrogen flames in the next sections.

N_2O emissions during unstable blowoff

During steady state experiments, while testing biogas at an equivalence ratio ($\phi \leq 0.9$) the biogas reactions become unstable, and a blowoff event occurred around sample 440. Fig. 2c shows the NO_x and N_2O trends during the blowoff event and the emission levels previous to that event. At blowoff, the NO emissions rapidly dropped to zero as the reactions were extinguished and the temperature drops. In low- NO_x combustor design, the minimum NO_x levels are often bound by the onset of combustion instability near LBO. As the flame temperature is decreased to reduce NO_x , the chemical reactions slow to the point where temperature becomes the rate limiting factor and the onset of LBO is triggered. However for the period of the blowoff event, the emissions of NO_2 rapidly increased from ~2 to 8 ppm and N_2O went from zero to 2 ppm. Since NG and biogas have no fuel nitrogen, it not be expected that these fuels emitted any N_2O .

Further examination of the blowoff emissions are shown in Fig. 3. Fig. 3a shows the history of NO_x and N_2O as a function of time (QCL gas analyzer). Fig. 3b zooms into the observed measurements the nitrogen species during the blowoff event, and Fig. 3c shows the scaled values of NO, NO_2 and N_2O to the total concentration of $\text{NO}_x + \text{N}_2\text{O}$. When NO reaches zero, the

fraction of N_2O hits a maximum point (2 ppm). The scaled results (Fig. 3c) show that, during stable operation, NO is around 95% of the total NO_x with NO_2 accounting for the remaining 5%, while N_2O remains zero or close to zero. At blowoff, NO drops to 0%, NO_2 reaches a maximum concentration of 80% with N_2O making up remaining 20%. The rapid production of NO_2 follows a fast destruction of the same species. Then a peak of N_2O follows NO_2 peak, indicating an exchange between these two species, as the reactions progress NO_2 is destroyed and N_2O is formed.

During the blowoff event ($440 < \text{sample} < 472$), the correlation coefficient for NO and NO_2 is -0.85 , which indicates the two species are strongly inversely correlated, i.e., the destruction of NO results in NO_2 . The coefficient for NO and N_2O was -0.09 showing no correlation; alternatively NO_2 and N_2O were positively but weakly correlated (0.67). Further, the correlation analysis of the N_2O destruction starting with the sample 463 shows a strong inverse correlation (-0.98) between N_2O and NO_2 , which indicates that N_2O is being destroyed while NO_2 is formed.

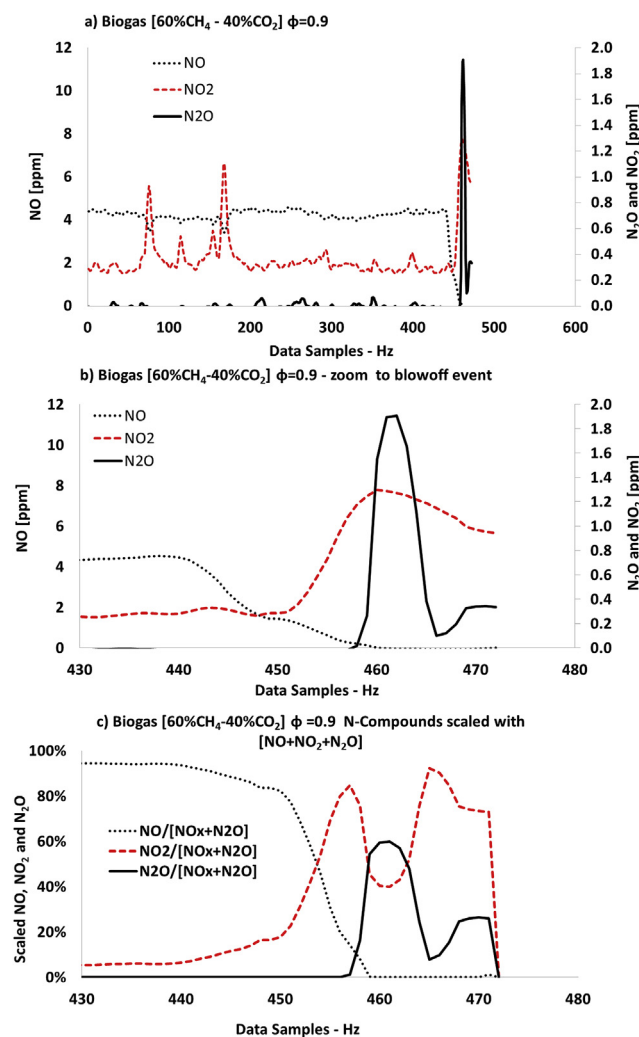


Fig. 3 – On-line exhaust measurements of NO_x and N_2O emissions for biogas flames at $\phi = 0.9$. a) Steady state at $\phi = 0.90$, b) zoom to blowoff event, c) Scaled percentage of $[\text{N_species}]/[\text{NO}_x + \text{N}_2\text{O}]$.

Emissions of N_2O during ignition and lean blowoff

This section presents the N_2O emissions resulting of transient events like the ignition and forced lean blowoff. It was observed experimentally that for NG, biogas and NG/hydrogen mixtures that a peak of N_2O follows the ignition and blowoff events. In general the LBO of premixed flames is characterized by a peak of carbon monoxide (CO) rather than a N_2O peak. Fig. 4 shows a typical result found for N_2O emissions during ignition and LBO with gaseous fuels. For ignition, either a diffusion hydrogen pilot flame or a spark plug was used. A significant peak of N_2O (12 ppm) was observed during the ignition event. Before ignition, the hydrogen pilot emits around 1 ppm of NO while NO_2 and N_2O remain negligible. Once the reactions are ignited and self-sustained, N_2O quickly disappears, while NO_2 and NO become the dominating species. It is noted that N_2O and NO don't coincide during any of these events. It is evident that at steady state, N_2O is a very reactive intermediate that is quickly destroyed before being emitted from a flame.

In sharp contrast, ignition and blowoff events are transient processes undergoing simultaneously chain-initiation/chain-propagating/chain-terminating reactions. In general it is complicated to develop physics-based correlations of blowout behavior by lack of understanding of the detailed phenomenology of the blowout process, such as the dynamics of near blowoff flames or the flame characteristics at the stabilization point. For example, disagreement about whether premixed flames in high turbulent intensity gas turbine environments have flamelet, “thickened” flamelet, or well stirred reactor (WSR)-like properties is evident in the literature. The dynamic nature has implications on blowout modeling as well as N_2O emission prediction, because the appropriate physical model clearly events changes depending whether the reaction zone exhibits flame sheet or volumetric characteristics [33].

N_2O emissions from hydrogen enriched natural gas flames

In this section, N_2O emissions from combustion of NG with up to 70% H_2 added by volume are examined. The time history of the results are shown in Fig. 5, which presents simultaneous variation of NO_x , N_2O and ϕ . The experiment was carried out by “stair stepping” ϕ from 0.45 to 0.72 and waiting for

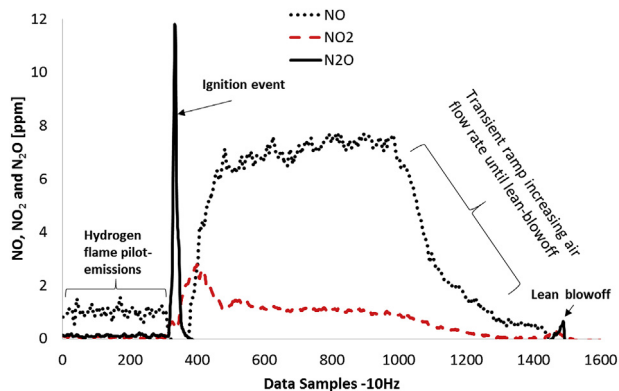


Fig. 4 – Typical exhaust emissions of NO_x and N_2O at ignition and LBO.

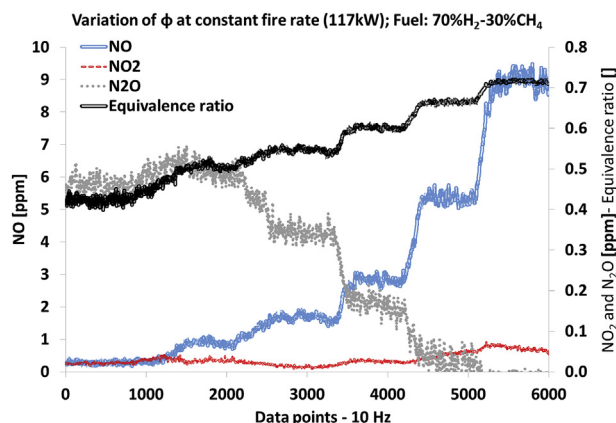


Fig. 5 – On-line exhaust measurements of NO_x , N_2O and ϕ for hydrogen enriched natural gas (70% H_2).

stabilization of emissions at each step. Within that range, the adiabatic flame temperature varies between 1440 and 1940 K, at $\phi = 0.45$ and $\phi = 0.72$, respectively.

The results indicate that the addition of hydrogen to NG stimulates direct emissions of N_2O . In particular the emissions of N_2O are inversely proportional to ϕ . The observed N_2O emissions from these premixed hydrogen enriched NG flames cannot be explained with the previous generalized assumption that low N_2O emissions result from the fast destruction reaction: $N_2O + H \rightarrow N_2 + OH$, rather than the slow formation reaction: $NH + NO \rightarrow N_2O + H$. Generally N_2O is a reactive intermediate in the flame that is consumed before reaching the atmosphere [37]. However, it seems that, under lean conditions, the hydrogen enriched NG flames promote the formation of N_2O . In hydrogen flames the route of formation of N_2O is through the NHi pathway $NH + NO \rightarrow N_2O + H$. In reactions lacking carbon species, the HCN pathway is not active. The results indicate that higher concentrations of H_2 , OH radicals and H atoms enhance the formation of N_2O through the NHi pathway. The results also show that the emissions of N_2O are more significant than those of NO_2 . The addition of hydrogen hinders the production of NO_2 maintaining it at very low levels ($NO_2 < 0.1$ ppm). In contrast NO and N_2O follow an inverse trend, with NO increasing with ϕ , and N_2O decreasing with increased ϕ . N_2O is rapidly consumed at high temperatures or when $\phi \sim 1$. The ultra-lean conditions seem to be responsible for the direct emissions of N_2O from the hydrogen enriched flames. The analysis of correlation between N_2O and ϕ is -0.94 , indicating a strong inverse correlation. At lower ϕ the N_2O levels rise, therefore lean conditions favor direct emissions of N_2O when NG is enriched with hydrogen up to 70% by vol. Furthermore the correlation between NO and N_2O is -0.91 demonstrating an inverse strong correlation; N_2O is high when NO is low and vice versa.

Chemical kinetics analysis

To help explain the observed results, multiple reaction mechanisms including the nitrogen chemistry were reviewed. Table 1 compiles every available N_2O pathway from five

Table 1 – Reaction pathways for the formation of N₂O according to six different reaction mechanisms.

Reaction#	Glarborg et al. (1998)	Miller-Bowman (1989)	GRI 3.0 (1999)	UCSD (2014)	Allen et al. (1995)	Baulch et al. (1994)
1	N ₂ O + M ↔ N ₂ + O + M	x	x	x	x	–
2	N ₂ O + H ↔ N ₂ + OH	x	x	x	x	–
3	N ₂ O + O ↔ 2NO	x	x	x	x	–
4	N ₂ O + OH ↔ N ₂ + HO ₂	x	x	x	x	–
5	NH + NO ↔ N ₂ O + H	x	x	x	x	x
6	NCO + NO ↔ N ₂ O + CO	x	x	–	–	x
7	CN + N ₂ O ↔ NCO + N ₂	x	–	–	–	–
8	NCO + NO ₂ ↔ CO ₂ + N ₂ O	–	x	–	–	–
9	N ₂ O + O ↔ N ₂ + O ₂	x	x	–	x	–
10	N ₂ O + OH ↔ HNO + NO	x	–	–	x	–
11	NNH + O ↔ N ₂ O + H	x	–	–	–	–
12	HNO + HNO ↔ N ₂ O + H ₂ O	x	–	–	x	–
13	N ₂ H ₂ + NO ↔ N ₂ O + NH ₂	x	–	–	–	–
14	CO + N ₂ O ↔ N ₂ + CO ₂	–	–	–	–	–
15	CH + N ₂ O ↔ HCN + NO	–	–	–	–	–
16	N ₂ O + NO ↔ NO ₂ + N ₂	–	–	–	x	–
17	CN + N ₂ O ↔ NCN + NO	–	–	N ₂ H + O ↔ N ₂ O + H	–	–
18	NCO + NO ₂ ↔ CO ₂ + N ₂ O	–	–	N ₂ O ↔ N ₂ + O	–	–
19	NH ₂ + NO ₂ ↔ N ₂ O + H ₂ O	–	–	–	–	NH ₂ + NO ↔ N ₂ O + H ₂
20	N ₂ O + OH ↔ HNO + NO	–	–	–	–	–
21	CN + NO ₂ ↔ CO + N ₂ O	–	–	–	–	–
22	NH + NO ₂ ↔ N ₂ O + OH	–	–	–	–	–
23	C + N ₂ O ↔ CN + NO	–	–	–	–	–

reaction mechanisms widely used for gaseous combustion applications (GRI 3.0 [35]; UCSD [36]; Glarborg et al., [38]; MillerBowman [39] and Allen et al., [40]). Five N₂O reaction pathways were found to be common to the five mechanisms: (1) N₂O(+M) ↔ N₂ + O(+M); (2) N₂O + H ↔ NO + NH; (3) N₂O + O ↔ 2NO; (4) N₂O + OH ↔ N₂ + HO₂ and (5) NH + NO → N₂O + H.

Out of the five mechanisms, the UCSD mechanism has been recently updated and includes seven pathways for the formation of N₂O [36]. In contrast the most complex mechanism by Glarborg et al., devises twenty-three possible pathways for the formation of N₂O. Given the simplicity of the GRI 3.0 and UCSD mechanisms, these two were tested in a Bragg Cell [34] with NG at variable excess of air (ϕ). Fig. 6 shows the modeled trends of CO and N₂O at variable ϕ (left) and includes experimental data of the of N₂O peaks in ppm measured during LBO with NG. The CO peak is typically observed close to the LBO limit and both reaction mechanisms can accurately

predict an analogous trend. Since the experiments indicated a release of N₂O when the reactions were close to the LBO limit, it was expected that the reaction mechanisms activated the N₂O pathways close to the leanest points. Fig. 6 compiles the numerical results for CO and N₂O at variable equivalence ratio with GRI 3.0 and UCSD. The N₂O and CO emissions modeled with the UCSD mechanism follows the experimental trends of N₂O and CO release at LBO. The UCSD mechanism predicts a maximum of ~3 ppm near LBO. This maximum is corresponding to the leanest point, when ϕ = 0.75.

Conversely, the N₂O trend obtained with GRI fails to predict the experimental trend. The trend predicted with GRI shows an inverse parabola, with N₂O increasing with excess air and reaches a maximum of 0.7 ppm around ϕ = 0.81. Further excess air reduces the amount of N₂O emitted. This result shows that, at low temperatures, GRI 3.0 is unable to predict the right N₂O trend. Further analysis of the production rates

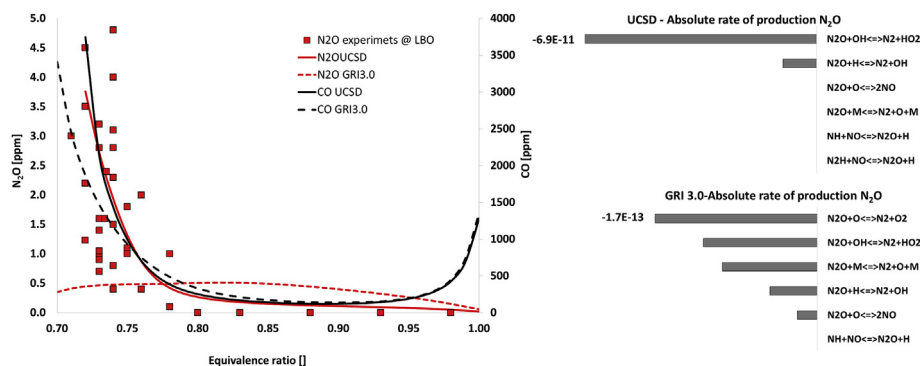


Fig. 6 – Modeled trends of N₂O and CO at variable ϕ with GRI 3.0 and UCSD mechanisms for 100% CH₄ (left); Absolute rate of production of N₂O near LBO limit (right).

were carried out at $\phi = 0.75$, where the maximum N_2O peak was observed with UCSD. The absolute rates of production of N_2O are shown in Fig. 6 (right). While UCSD shows that the main route of formation of N_2O is through the reactions: $N_2O + OH \leftrightarrow N_2 + HO_2$ and secondarily through $N_2O + H \leftrightarrow N_2 + OH$. The absolute rate of production of N_2O predicted with GRI indicates that N_2O is being formed through these same reactions plus three additional reactions $N_2O + O \leftrightarrow N_2 + O_2$, $N_2O(+M) \leftrightarrow N_2 + O(+M)$ and $N_2O + O \leftrightarrow 2NO$. These results seem to indicate that the reactions of molecular N_2 with hydroperoxyl (HO_2) are fundamental for the conversion of N_2 into N_2O at low temperatures. Furthermore, both UCSD and GRI show that N_2O is also formed through the combination of N_2 with OH radical and in a lesser importance through the reaction with a third body [M], $N_2O(+M) \leftrightarrow N_2 + O(+M)$. Interestingly none of these routes is described in neither the NCO or NH_3 routes, which according to the literature are the main routes to produce N_2O in homogeneous combustion of fossil fuels: $NCO + NO \rightarrow N_2O + CO$ and $NH + NO \rightarrow N_2O + H$. The results of these reactions mechanism indicate the reactions of CH_4 at LBO release N_2O through the reactions: $N_2O + OH \leftrightarrow N_2 + HO_2$ and to a lesser extent through $N_2O + H \leftrightarrow N_2 + OH$, although further experimental analysis must be carried out to confirm the kinetics of N_2O at low temperatures.

Conclusions

The experimental results presented in this paper indicate that, under steady state conditions, the combustion of NG and biogas does not emit N_2O , which is consistent with previous studies. However, during ignition, unstable blowoff and LBO events, the emissions of N_2O and NO_2 are significant whereas the emission of NO is zero.

The addition of hydrogen to the fuel enhances the emissions of N_2O . While the behavior of NO follows ϕ in a typical fashion (NO increases when ϕ increases (for $\phi < 1$), N_2O is inversely proportional to ϕ and is promoted at leaner conditions (at lower ϕ). At lean conditions the emissions of N_2O are more significant than the emission of NO_2 , which remains at <0.1 ppm. These trends are not observed with any other gaseous fuels such as NG or biogas.

The UCSD reaction mechanism is able to accurately predict the N_2O and CO trends at LBO. On the other hand, GRI 3.0 fails to predict an accurate trend for N_2O and only reasonable levels of CO are observed at LBO. Further analysis of the reactions indicates that the combustion reactions of CH_4 at LBO release N_2O mainly through the reactions: $N_2O + OH \leftrightarrow N_2 + HO_2$ and $N_2O + H \leftrightarrow N_2 + OH$. None of these reactions is included in the previously known NH_3 or NCO pathways for the formation of N_2O in homogeneous combustion.

The experimental results suggest that, for ultra-lean combustion systems that are being adopted for low NO_x emissions performance, certain operations may give rise to non-trivial emissions of N_2O . This is particularly true for systems that must follow load and see large numbers of starts/stops. Such systems may become more important as the need arises to stabilize a grid supplied with increasing amounts of intermittent renewable power.

Acknowledgements

The Authors acknowledge the support of the California Energy Commission (Contract 500-13-004). The support of Colciencias-Colombia through Francisco Jose Caldas Scholarship is gratefully acknowledged. The assistance of D. Avila and N. Kirksey during the experiments is thankfully appreciated. Horiba Instruments provided the MEXA 1400 instrument and associated training for its proper use.

REFERENCES

- [1] IPCC. *Climate change 2007: the physical science basis contribution of working group I to the fourth assessment report of the intergovernmental panel on climate change*. Cambridge, United Kingdom and New York: Cambridge University Press; 2007. 2007.
- [2] Smith K. Introduction. In: Smith K, editor. *Nitrous Oxide and Climate Change*. London: Earthscan; 2010. p. 1–3.
- [3] Galloway JN, Aber JD, Erisman JW, Seitzinger SP, Howarth RW, Cowling EB, et al. The nitrogen cascade. *BioScience* 2003;53(4):341–56.
- [4] Smith K, Crutzen P, Mosier A, Winiwarter W. The global nitrous oxide budget: a reassessment. In: Smith K, editor. *Nitrous oxide and climate change*. London, Washington DC: Earthscan; 2010. p. 63–84.
- [5] Banin A. Global budget of N_2O : the role of soils and their change. *Sci Total Environ* Nov. 1986;55:27–38.
- [6] Li M, Shimizu M, Hatano R. Evaluation of N_2O and CO_2 hot moments in managed grassland and cornfield, southern Hokkaido, Japan. *CATENA* Oct. 2015;133:1–13.
- [7] Prather MJ, Holmes CD, Hsu J. Reactive greenhouse gas scenarios: systematic exploration of uncertainties and the role of atmospheric chemistry. *Geophys Res Lett* 2012;39(9):6–10.
- [8] Armesto L, Boerrigter H, Bahillo A, Otero J. N_2O emissions from fluidised bed combustion. The effect of fuel characteristics and operating conditions. *Fuel* Oct. 2003;82(15–17):1845–50.
- [9] Kramlich JC, Linak WP. Nitrous oxide behavior in the atmosphere, and in combustion and industrial systems. *Prog Energy Combust Sci* 1994;20(2):149–202.
- [10] Muzio LJ, Montgomery TA, Samuelsen GS, Kramlich JC, Lyon RK, Kokkinos A. Formation and measurement of N_2O in combustion systems. *Symposium Int Combust* 1991;23(1):245–50.
- [11] Kramlich JC, Cole JA, McCarthy JM, Lanier WS, McSorley JA. Mechanisms of nitrous oxide formation in coal flames. *Combust Flame Sep.* 1989;77(3–4):375–84.
- [12] Valentim B, Lemos de Sousa MJ, Abelha P, Boavida D, Gulyurtlu I. Combustion studies in a fluidised bed—the link between temperature, NO_x and N_2O formation, char morphology and coal type. *Int J Coal Geol Jun.* 2006;67(3):191–201.
- [13] Saikaew T, Supudommak P, Mekasut L, Piumsomboon P, Kuchonthara P. Emission of NO_x and N_2O from co-combustion of coal and biomasses in CFB combustor. *Int J Greenh Gas Control Sep.* 2012;10:26–32.
- [14] de las Obras-Loscertales M, Mendiara T, Rufas A, de Diego LF, García-Labiano F, Gayán P, et al. NO and N_2O emissions in oxy-fuel combustion of coal in a bubbling fluidized bed combustor. *Fuel Jun.* 2015;150:146–53.
- [15] Zhou H, Huang Y, Mo G, Liao Z, CEN K. Conversion of fuel-N to N_2O and NO_x during coal combustion in combustors of different scale. *Chin J Chem Eng Sep.* 2013;21(9):999–1006.

- [16] Svoboda K, Pohorelý M. Influence of operating conditions and coal properties on NO_x and N₂O emissions in pressurized fluidized bed combustion of subbituminous coals. *Fuel* May 2004;83(7–8):1095–103.
- [17] Deng L, Jin X, Zhang Y, Che D. Release of nitrogen oxides during combustion of model coals. *Fuel* 2016;175:217–24.
- [18] Zhou H, Huang Y, Mo G, Liao Z, Gen K. Experimental investigations of the conversion of fuel-N, volatile-N and char-N to NO_x and N₂O during single coal particle fluidized bed combustion. *J Energy Inst* 2016. <http://dx.doi.org/10.1016/j.joei.2015.10.006>.
- [19] G. Karavalakis, M. Hajbabaie, T. D. Durbin, K. C. Johnson, Z. Zheng, y W. J. Miller, “The effect of natural gas composition on the regulated emissions, gaseous toxic pollutants, and ultrafine particle number emissions from a refuse hauler vehicle”, *Energy*, no 0.
- [20] Hashemi SA, Fattahi A, Sheikhzadeh GA, Mehrabian MA. Investigation of the effect of air turbulence intensity on NO_x emission in non-premixed hydrogen and hydrogen-hydrocarbon composite fuel combustion. *Int J Hydrogen Energy* 2011;36(16):10159–68.
- [21] Lee K, Kim H, Park P, Yang S, Ko Y. CO₂ radiation heat loss effects on NO_x emissions and combustion instabilities in lean premixed flames. *Fuel* 2013;106:682–9.
- [22] C. E. Baukal, J. Z. Co, y E. Apache, “Air preheat effects on NO_x”, pp. 1–10.
- [23] Rutar T, Malte PC, Kramlich JC. Investigation of NO_x and CO formation in lean-premixed, methane/air, high-intensity, confined flames at elevated pressures. *Proc Combust Inst* 2000;28(2):2435–41.
- [24] Naha S, Aggarwal SK. Fuel effects on NO_x emissions in partially premixed flames. *Combust Flame Oct*. 2004;139(1–2):90–105.
- [25] Cheng RK, Littlejohn D, Strakey PA, Sidwell T. Laboratory investigations of a low-swirl injector with H₂ and CH₄ at gas turbine conditions. *Proc Combust Inst* 2009;32(2):3001–9.
- [26] Rørtveit GJ, Zepter K, Skreiberg Ø, Fossum M, Hustad JE. A comparison of low-NO_x burners for combustion of methane and hydrogen mixtures. *Proc Combust Inst* 2002;29(1):1123–9.
- [27] Tseng C. Effects of hydrogen addition on methane combustion in a porous medium burner. *Int J Hydrogen Energy Jun*. 2002;27(6):699–707.
- [28] Dutka M, Ditaranto M, Løvås T. NO_x emissions and turbulent flow field in a partially premixed bluff body burner with CH₄ and H₂ fuels. *Int J Hydrogen Energy* 2016;41(28):12397–410.
- [29] Gao X, Duan F, Lim SC, Yip MS. NO_x formation in hydrogen–methane turbulent diffusion flame under the moderate or intense low-oxygen dilution conditions. *Energy* 2013;59:559–69.
- [30] Geddes JA, Murphy JG. 10 – the science of smog: a chemical understanding of ground level ozone and fine particulate matter. *Metrop Sustain* 2012:205–30.
- [31] Cheng RK, Littlejohn D, Nazeer WA, Smith KO. Laboratory studies of the flow field characteristics of low-swirl injectors for application to fuel-flexible turbines. *J Eng Gas Turbines Power* 2008;130(2):21501–11.
- [32] Johnson MR, Littlejohn D, Nazeer WA, Smith KO, Cheng RK. A comparison of the flowfields and emissions of high-swirl injectors and low-swirl injectors for lean premixed gas turbines. *Proc Combust Inst* 2005;30(2):2867–74.
- [33] Lieuwen T, McDonell V, Santavicca D, Sattelmayer T. Burner development and operability issues associated with steady flowing syngas fired combustors. *Combust Sci Technol May* 2008;180(6):1169–92.
- [34] Bragg SL. Application of reaction rate theory to combustion chamber analysis. *Aeronautical Res Counc* 1953:1629–33.
- [35] G. P. Smith, D. M. Golden, M. Frenklach, N. W. Moriarty, B. Eiteneer, M. Goldenberg, C. T. Bowman, R. K. Hanson, S. Song, J. William C. Gardiner, V. V. Lissianski, y Z. Qin, “GRI-MECH 3.0”, http://www.me.berkeley.edu/gri_mech/.
- [36] “Chemical-Kinetic Mechanisms for Combustion Applications, San Diego Mechanism web page, Mechanical and Aerospace Engineering (Combustion Research), University of California at San Diego (<http://combustion.ucsd.edu>)”.
- [37] Hayhurst AN, Lawrence AD. Emissions of nitrous oxide from combustion sources. *Prog Energy Combust Sci* 1992;18(6):529–52.
- [38] Glarborg P, Alzueta MU, Dam-Johansen K, Miller JA. Kinetic modeling of hydrocarbon/nitric oxide interactions in a flow reactor. *Combust Flame Oct*. 1998;115(1–2):1–27.
- [39] Miller JA, Bowman CT. Mechanism and modeling of nitrogen chemistry in combustion. *Prog Energy Combust Sci* 1989;15(4):287–338.
- [40] Allen M, Yetter R, Dryer YF. The decomposition of nitrous oxide at 1.5–10.5 atm and 1103–1173 K. *Int J Chem Kinet* 1995;27(9):883–909.